Proceedings of ASME Turbo Expo 2014: Turbine Technical Conference and Exposition
GT2014
June 16 – 20, 2014, Düsseldorf, Germany

GT2014-25385

TURBOMACHINERY FLOWPATH DESIGN AND PERFORMANCE ANALYSIS FOR SUPERCRITICAL CO2

Dr. Leonid Moroz
SoftInWay Inc.
15 New England Executive Park
Burlington, MA 01803, USA
L.Moroz@softinway.com

Dr. Boris Frolov
SoftInWay Inc.
15 New England Executive Park
Burlington, MA 01803, USA
boris.frolov@softinway.com

Dr. Maksim Burlaka
SoftInWay Inc.
15 New England Executive Park
Burlington, MA 01803, USA
M.Burlaka@softinway.com

Oleg Guriev
SoftInWay Inc.
15 New England Executive Park
Burlington, MA 01803, USA
O.Guryev@softinway.com

ABSTRACT

The development of Supercritical CO2 (S-CO2) power cycles is currently a major focus of the engineering and scientific community. The reason for such a growing interest in this type of power can be explained by the significant benefits in size and efficiency of power cycles, which use S-CO2 as a working fluid, as compared to conventional steam power generation. Many areas of application such as nuclear, solar, waste heat, energy storage, and clean coal combustion, are being studied for S-CO2 power production. Most of the publications discussing S-CO2 are concentrated on optimization of the cycle's thermodynamic characteristics, topping and bottoming and have been conceptualized based on the heat source. At the same time, numerous aspects of turbomachinery design are often overlooked or are not well understood. This article discusses some specific engineering aspects of the design of turbine flow path which uses S-CO2 as a working fluid. The following design options have been studied to determine the best turbine configuration: number of stages, rotational speed, impulse versus reaction, types of stages, and radial clearance influence. The effect of larger bending loads, resulting from high power density on nozzles and blade chords size and, consequently, turbine length, has also been studied. The authors hope that the results presented in the article will help the engineering community design better S-CO2 turbomachinery.

INTRODUCTION

For this paper, important turbine configuration characteristics are explored, which impact cycle efficiency, specifically focusing on the S-CO2 cycle. Beginning with an overview of current publications and studies already performed, it is clear to see that the S-CO2 cycle is gaining popularity and has developed quite a following in recent years.

Some key advantages of the S-CO2 cycle include:

1) Higher cycle efficiency compared to a Helium Brayton system. This is the result of lower compressor work due to the fact that the cold end of the loop operates at temperatures and pressures near a critical point of CO2, which results in fast density and specific heat increase.
2) S-CO2 Brayton cycle eliminates the need to deal with sodium-water reactions in the licensing and safety evaluation which makes them more attractive than superheated and supercritical steam cycles.
3) The CO2 temperature profile in the supercritical region can provide a better match to the heat source temperature glide; therefore "pinching" can be avoided.
4) Better stability and minimal environmental impact and cost, as compared to using ORC fluids.

In the chart below, we can look at the different cycles and their performance as a factor of inlet temperature versus cycle efficiency. Here it becomes quite clear that the S-CO2 cycle has an advantage over superheated and supercritical steam cycles starting at 550° C. Also, when temperatures are in the 450-550° C range, it may still be advantageous due to smaller size and manufacturing cost.

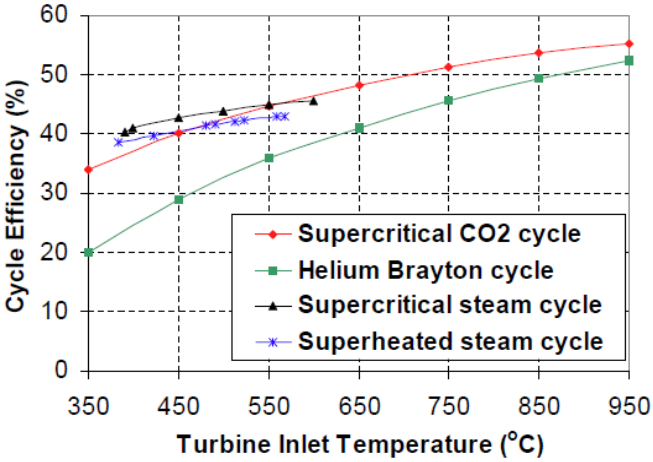

Fig. 1. Cycle efficiency comparison of advanced power cycle [4].

For S-CO2 turbines developed at conceptual and preliminary levels, main design features such as axial length and the number of stages and diameters were determined to be significantly less based on only thermo/aerodynamic design criteria [1, 2, 3, 4, 6, 10, 11, and 12].

For example, the detailed major component, system design evaluation and multiple parameter optimizations have been performed by the family of supercritical CO2 Brayton power cycles for application to advanced nuclear reactors and presented in [4]. The turbomachinery design was performed for the direct supercritical CO2 recompression cycle and proved to be very compact and achieved high efficiencies. For the 600 MW_{th}/246 MW_e power plants, the 3 stage axial turbine body was 1.2m in diameter and only 0.55m long.

The [2] presents the discussion of several possible ways of S-CO2 for SFR performance improvement. One set of options incorporates optimization approaches, such as variations in the maximum and minimum cycle pressure and minimum cycle temperature, as well as a tradeoff between the component sizes and the cycle performance. In addition, it also covers options which have received little to no attention in the previous studies. Specific options include a "multiple-recompression" cycle configuration, intercooling and reheating, as well as liquid-phase CO2 compression (pumping) either by CO2 condensation or by a direct transition from the supercritical to the liquid phase. The turbine sizing showed that the 3 stage turbine was around 0.5m length and 0.8m diameter.

In some articles the small cycles (up to 10 MW) and small scale power plants are discussed. Therefore the turbomachinery used was of radial type due to small volume flow rates.

It is unclear in these published works whether they have taken into account only thermo/aerodynamic criteria or if structural constraints were even a part of the analysis. This is why we feel it is necessary to perform a complete analysis of an S-CO2 turbine taking into account both the thermo/aerodynamic requirements and structural restraints.

In this article, some specifics to S-CO2 high density fluid aerodynamics and structural aspects of turbine design were studied based on the Simple Brayton cycle scheme for 100MW net electrical output sodium-cooled fast reactor, presented in [4]. The main Simple Brayton cycle parameters, and those required for turbine design, were determined with a heat balance calculation tool called AxCYCLE™ [7]. The reactor's core temperature is higher than 500°C [4], but because of temperature losses in the intermediate contour, the heat exchanger outlet temperature was set as 480° C. The Simple Brayton cycle scheme is presented in Figure 2 below.

As a result of cycle heat balance analysis, the overall cycle parameters required for turbine design have been determined as follows:

Electrical power production - 100 MW
Thermal efficiency - 31.54%
Reactor outlet pressure - 21 MPa
Reactor outlet temperature - 753 K

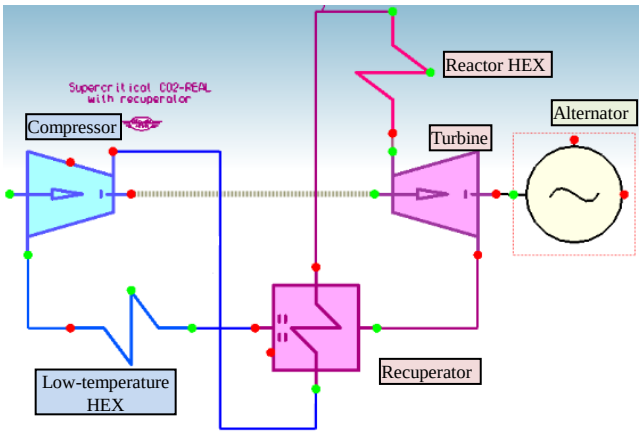

Fig. 2. Closed Brayton cycle with recuperator.

The turbine has to be designed for the next set of boundary conditions:

Inlet total pressure - 21 MPa
Inlet total temperature - 753 K
Mass flow rate – 1270.5 kg/s
Outlet static pressure – 7.35 MPa

The turbine performance and configuration has been studied with regards to major design options:

1. stage type – impulse vs. reaction
2. number of stages
3. rotational speed
4. radial clearance variation
5. Structural limitations

All design steps, thermo/aerodynamic and structural analyses were performed within the AxSTREAM™ turbomachinery design & optimization tool [5,7,8,9].

Over this study, the 1D meanline codes (direct task and inverse task [7, 8]) were used for thermodynamic calculations. Beam theory was applied as the structural calculation method.

NOMENCLATURE

L – rotor length, m
D – rotor hub diameter, m
OD – outer diameter, m
N – power, MW
η_{ts} – turbine total-to-static efficiency, -
H_{ts} - turbine total-to-static heat drop, kJ/kg
G – mass flow rate, kg/s
K - safety factor, -
σ – strength limit, MPa

Subscripts

t – yield
lt – long time (rupture)
cr – creep

STAGES NUMBER EFFECT

Based on only aerodynamic performance criteria, the impulse and reaction types of flow paths were studied. The same seal configuration and clearances (Clr=0.001*OD) have been assumed at this step for both types of flow paths. In this study, the number of stages serves as a main design parameter, against which the turbine performance was analyzed. The other turbine parameters, such as the hub diameter, flow angle and rotational speed, were found as a result of thermo/aerodynamic optimization to achieve the highest possible performance for a given number of stages. This study is also useful to understand how the type and number of stages affect turbine axial length. The large number of design solutions have been generated and analyzed with regards to the turbine performance. The influence of the stages' numbers on turbine total-to-static efficiency is presented in Figure 3.

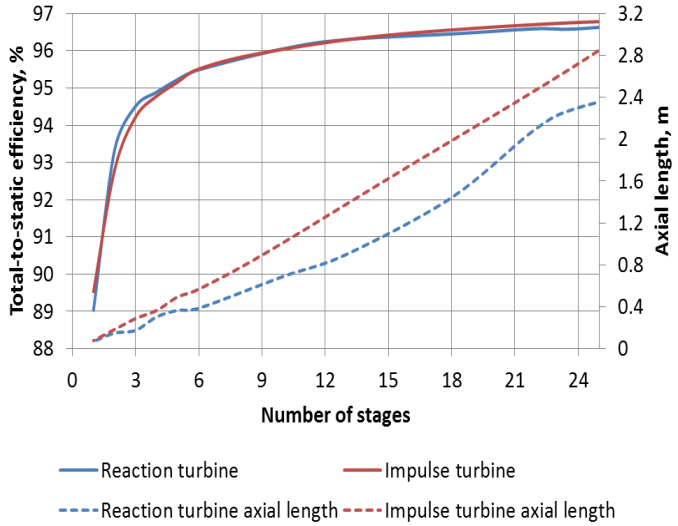

Fig. 3. Turbine efficiency and axial length vs. number of stages.

It is evident from the chart, that analysis has not detected advantages in performance for any of the studied variants with assumed seal options, but demonstrated some advantages in axial length for reaction types. It should be noted again, that the result, presented in Figure 3 for a different number of stages, has been obtained with a variable rotational speed, which differs from generator frequencies for 50Hz or 60Hz electrical grids. It is clear that in real design, only one design solution corresponding to 50Hz or 60Hz rotational speed can be implemented and it is also interesting to learn how rotational speed affects turbine performance. The results of this study, in terms of turbine performance versus rotational speed are presented in Figure 4. The total number of studied solutions was approximately 1000 for each impulse and reaction turbine type.

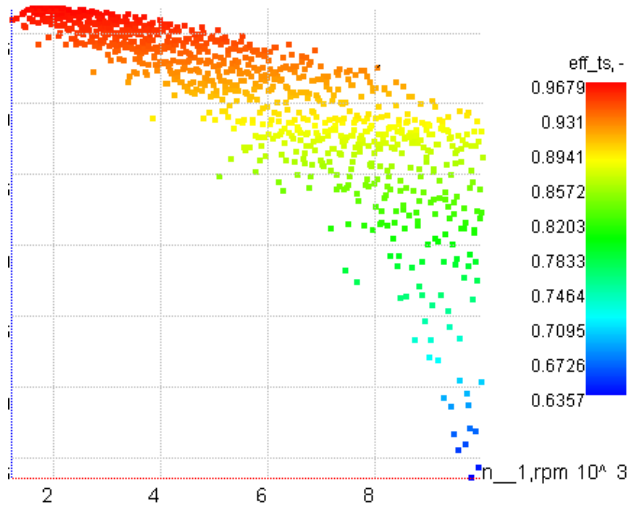

Fig. 4. Total-to-static efficiency vs. rotational speed for impulse turbine

Each point on Figure 4 represents design solutions with different hub diameters, number of stages, and flow angles. But, similar to the first case, from this chart we can observe general trends with regard to rotational speed. The variants with 3000 and 3600 RPM, corresponding to 50Hz or 60Hz frequencies, demonstrate not the highest possible level of performance, but are very close to best solution.

Further design steps and analyses to determine types of flow path and number of stages were completed based on more specific definition of rotational speed and turbine diameter.

To evade additional costs and design complexity (the necessity of reduction/multiplication gear), the rotational speed has been fixed to 3000 RPM.

Considering both general structural limitations on the turbine diameter and results from [4] the preliminary defined geometry of the power conversion unit, the hub diameter was determined equal to 825 mm, the same for both impulse and reaction turbines.

STAGE TYPE SELECTION

After the application of design limitations from the previous chapter, two variants of turbines have been designed – impulse and reaction – with corresponding levels of reaction and design features. Each turbine type turned out to have its own clear optimum, with regards to the number of stages.

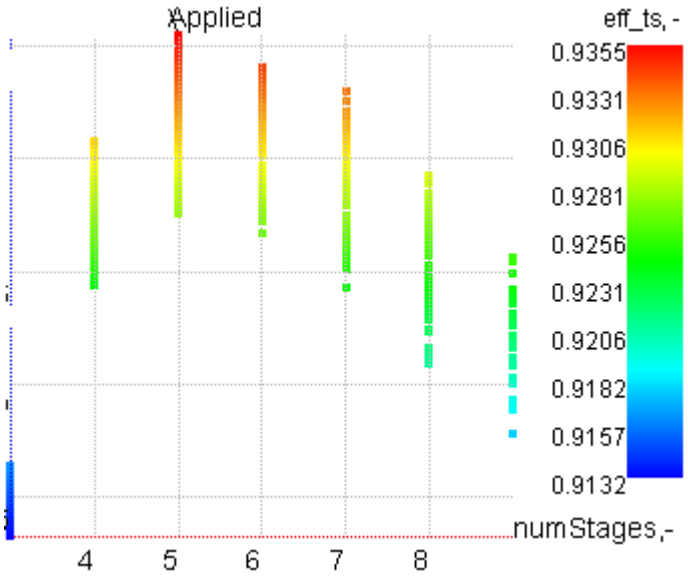

Fig. 5. Total-to-static efficiency (eff_ts) vs. number of stages (numStages) for impulse turbine

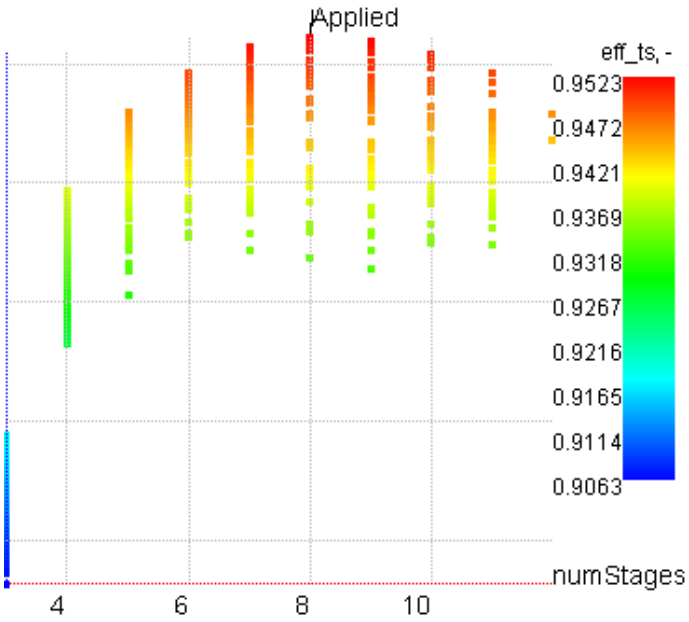

Fig. 6. Total-to-static efficiency (eff_ts) vs. number of stages (numStages) for reaction turbine

The results, presented in Figure 5 and Figure 6 show that the highest possible efficiency can be achieved with 5 stages for impulse type and 8 stages for reaction type. These two competing variants of reaction and impulse turbines were selected for further study. Their integral parameters, axial load and overall dimensions are presented in Table 1 and Figure 7.

Tab. 1. Impulse and reaction turbines integral parameters

	Impulse	Reaction
Stages number, -	5	8
η_{ts}, %	93.69	95.50
N, MW	159.5	162.25
Axial load, MN	0.55	1.91
Axial length, mm	589	762
Maximal tip diameter, mm	1060	1110

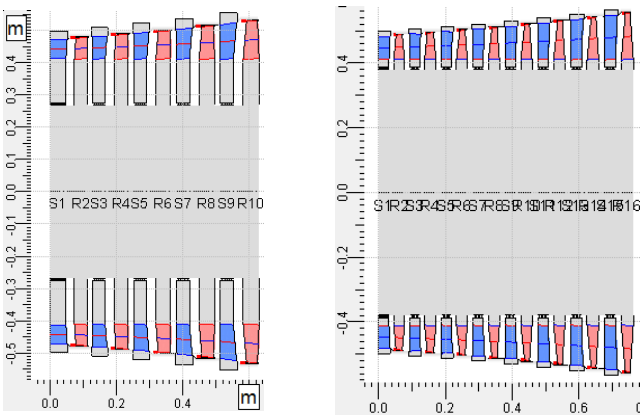

Fig. 7. Two variants of designed flow paths meridional view

For specified speed and diameter, we now can observe some difference in efficiency, axial load and size between two competing variants. The reaction variant demonstrates about 2% higher efficiency, comparing to impulse, but larger axial length. But its 3 additional stages will cause additional manufacturing cost. Its rate will depend on manufacturing capabilities per OEM. The axial load of the reaction type turbine is also about 3 times larger than that of the impulse type. Such a difference may result in additional measures to reduce thrust bearing load; for instance, a bigger balance piston size, which in turn can cause greater shaft end seal leakages.

EFFECT OF RADIAL CLEARANCES

The effect of the seal clearance's size on turbine performance is commonly known in turbomachinery society. For this specific study we determined to evaluate how significant the effect of flow path type is on performance. Two competing variants were analyzed with the same tip and root seal configuration – high-low lab seal with 2 teeth, but different clearance sizes, varying from 0 up to 2.5 mm. The total-to-static efficiency versus the clearance size is presented in Figure 8.

The efficiency was calculated using next equation:

$$\eta_{ts} = \frac{N}{G \cdot H_{ts}}$$

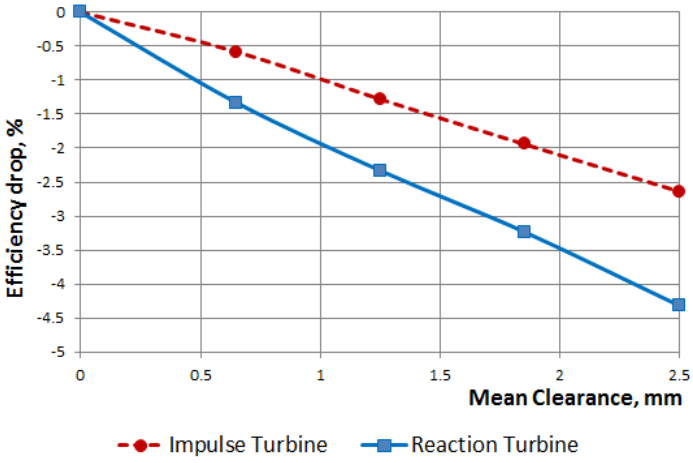

Fig. 8. Turbine efficiency drop due to clearances increase.

The efficiency drop was caused by power decrease due to omitting by part of the fluid the blade channel (leakage). It demonstrates to be almost linear against the clearance sizes within a studied range. The reaction type shows a two times higher efficiency drop and requires more attention from designers to seal tip and root leakages. The higher sensitivity of the reaction turbine to the radial clearance is due to the higher reaction (pressure difference) at the blade tip, which in turn leads to higher leakages for the same seals.

It should be noted that due to high power density of S-CO2 turbines, even low leakage leads to significant power drop. In fact, reducing the leakages and sealing design is one of the most important concerns for design of S-CO2 turbines. See Figure 6.

For further performance comparison, the clearances were set at 1mm for all stages of both reaction and impulse type turbines.

STRUCTURAL ASPECTS CONSIDERATION

Due to the high fluid density resulting in the higher power density, the aerodynamic loads on nozzles and blades are significantly higher than those of regular steam or gas turbines. Consequently, the structural aspects are of significant importance in order to determine turbine configurations with aerodynamic aspects and must be studied thoroughly for each design.

The structural calculations were performed for both variants for X12Cr13 alloy, which is a typical material for steam turbine blades in a temperature range of up to 813 K. The temperature range for this particular turbine design varies from 630 K to 753 K.

Material properties for variable temperatures are presented in the Table 2.:

Tab. 2. Material properties

Temperature, K	Elasticity modulus, MPa	Yield strength, MPa	Long time (creep rupture) strength limit, MPa	Creep strength limit, MPa
293.1	2.17E+05	570	560	550
473.1	2.12E+05	530	520	510
573.1	2.06E+05	510	500	490
673.1	1.98E+05	460	450	440
773.1	1.89E+05	440	430	420
873.1	1.80E+05	310	300	290

Structural calculation approaches and results are presented below:

Based on a particular temperature for each blades row, the allowable stress limits were defined as follows:

1) The calculation of allowable stresses $[\sigma]$ for each strength limit is performed by the dividing of strength limits on respective safety factor:

$$[\sigma]=\frac{\sigma_t}{K_t};\ [\sigma]=\frac{\sigma_{lt}}{K_{lt}};\ [\sigma]=\frac{\sigma_{cr}}{K_{cr}},\ \text{where}$$

σ_t – yield strength at operating temperature;

σ_{lt} – long-time strength limit for 100000 hours,

σ_{cr} – creep strength limit at 1% deformation for 100000 hours;

K_t, K_{lt}, K_{cr} – respective safety factors.

2) The minimal value among these three values is used as an allowable stress value.

Rotor blade bending stresses should satisfy the following condition:

$\sigma_{\max.bend} < [\sigma]/K_{bend}$,where

$\sigma_{\max.bend}=\max\{\sigma_{ss},\sigma_{l.e},\sigma_{t.e}\}$ – maximum bending stress; $\sigma_{ss},\sigma_{l.e},\sigma_{t.e}$ - suction side, leading edge, trailing edge stress; K_{bend} – blade bending stress safety factor.

Structural analysis has been completed firstly for each variant of turbines based on aerodynamic criteria only. The stresses were found to be significantly higher than the allowable limits for both impulse and reaction types.

For the impulse turbine, for instance, the actual stresses in nozzles exceeded the allowable ones by more than 3 times and 1.6 times for bucket. For the reaction turbine the excess of actual stresses above allowable ones was even higher (3.65 for nozzle and 4.7 for bucket).

The detailed data on stresses for this variant of flow path geometry is presented in Table 3.

Tab. 3. Detailed data on stresses for turbine geometry optimized based on aerodynamic approach only.

	Chord, mm	Allowable tensile stress $[\sigma]$, MPa	Calculated tensile stresses, MPa	Allowable bending stress $[\sigma]/K_{bend}$, MPa	Calculated maximum bending stresses, MPa
Impulse turbine					
1st nozzle	84.3	-	-	217.0	1085.8
1st bucket	40.1	218.8	19.5	43.8	149.0
2nd nozzle	89.2	-	-	219.4	1002.0
2nd bucket	43.2	221.1	21.7	44.2	149.5
3rd nozzle	92.6	-	-	221.8	862.4
3rd bucket	45.2	223.5	23.8	44.7	157.2
4th nozzle	96.4	-	-	224.2	680.3
4th bucket	46.9	227.3	26.4	45.5	173.8
5th nozzle	84.3	-	-	229.0	604.5
5th bucket	40.1	233.3	29.4	46.7	200.5
Reaction turbine					
1st nozzle	48.1	-	-	217.0	1268.0
1st bucket	43.2	217.7	16.2	43.5	336.8
2nd nozzle	50.4	-	-	218.5	1928.7
2nd bucket	45.0	219.3	17.0	43.9	312.0
3rd nozzle	50.8	-	-	220.1	1827.9
3rd bucket	45.8	220.8	24.2	44.2	974.4
4th nozzle	51.9	-	-	221.6	1496.7
4th bucket	46.8	222.3	26.1	44.5	1100.7
5th nozzle	53.2	-	-	223.1	1447.7
5th bucket	47.2	223.8	27.5	44.8	1332.7
6th nozzle	53.7	-	-	224.7	1354.5
6th bucket	48.3	225.7	30.0	45.1	1892.8
7th nozzle	55.2	-	-	228.0	1290.1
7th bucket	49.5	229.5	32.1	45.9	2403.9
8th nozzle	56.7	-	-	231.8	1289.1
8th bucket	51.3	233.2	34.9	46.6	1900.0

The detailed information on stresses has been analyzed and both turbines have been redesigned with an optimization procedure, which considers both aerodynamic and structural aspects, and new nozzles/blades numbers and chords sizes were determined. In this variant of turbine geometry, the nozzles/blades numbers and chords were determined to have actual stresses satisfying the allowable limits.

The through flow meanline aero-structural optimization algorithm is integrated into the turbomachinery design tool (AxSTREAM). Its goal is to find the maximum efficiency value while satisfying the structural limitations (the value of chords for which actual stresses will be lower than allowable). The search is performed with the Monte Carlo method:

1) Variants with different chords are created. The values of chords are generated arbitrarily in some specified range
2) The optimal (from an aerodynamic point of view) number of airfoils is calculated to satisfy the optimum

pitch criterion for minimum profile losses and aerodynamic calculation

3) Structural analysis is performed
4) The solution that satisfies structural limitations and has the best performance is selected as the final solution

After the optimization, the value chords were increased significantly to satisfy the structural requirements. For the aerodynamic analysis, simple meanline code was used and for structural analysis, 1D beam theory.

The detailed data on stresses for this structurally optimized variant of flow path geometry are presented in Table 4.

Tab. 4. Detailed data on stresses, for turbines geometry, optimized, based on structural and aerodynamic approach

	Chord, mm	Allowable tensile stress $[\sigma]$, MPa	Calculated tensile stresses, MPa	Allowable bending stress $[\sigma]/K_{bend}$, MPa	Calculated maximum bending stresses, MPa
Impulse turbine after the Aerodynamic-Structural optimization					
1st nozzle	173.9	-	-	217.0	216.6
1st bucket	74.3	218.8	19.39	43.8	43.2
2nd nozzle	187.8	-	-	219.4	211.1
2nd bucket	81.0	221.1	21.9	44.2	44.0
3rd nozzle	167.5	-	-	221.8	220.5
3rd bucket	86.2	223.5	23.7	44.7	44.6
4th nozzle	175.2	-	-	224.2	188.0
4th bucket	94.2	227.3	26.2	45.5	44.2
5th nozzle	158.8	-	-	229.0	201.7
5th bucket	101.7	233.3	29.1	46.7	46.6
Reaction turbine after the Aerodynamic-Structural optimization					
1st nozzle	95.0	-	-	217.0	210.6
1st bucket	108.3	217.7	16.5	43.5	43.2
2nd nozzle	131.0	-	-	218.5	220.4
2nd bucket	88.3	219.3	26.2	43.9	40.5
3rd nozzle	136.5	-	-	220.1	219.5
3rd bucket	130.0	220.8	19.1	44.2	44.0
4th nozzle	92.9	-	-	221.6	213.1
4th bucket	215.8	222.3	34.4	44.5	43.9
5th nozzle	93.1	-	-	223.1	220.1
5th bucket	226.6	223.8	38.6	44.8	44.7
6th nozzle	86.2	-	-	224.7	213.1
6th bucket	257.0	225.7	47.9	45.1	45.5
7th nozzle	79.9	-	-	228.0	222.2
7th bucket	250.8	229.5	49.6	45.9	45.6
8th nozzle	85.4	-	-	231.8	204.8
8th bucket	270.8	233.2	53.8	46.6	43.2

The comparison of two competing flow path axial dimensions before and after the aero-structural optimization is shown on Figure 9 and in Tables 5 and 6 below.

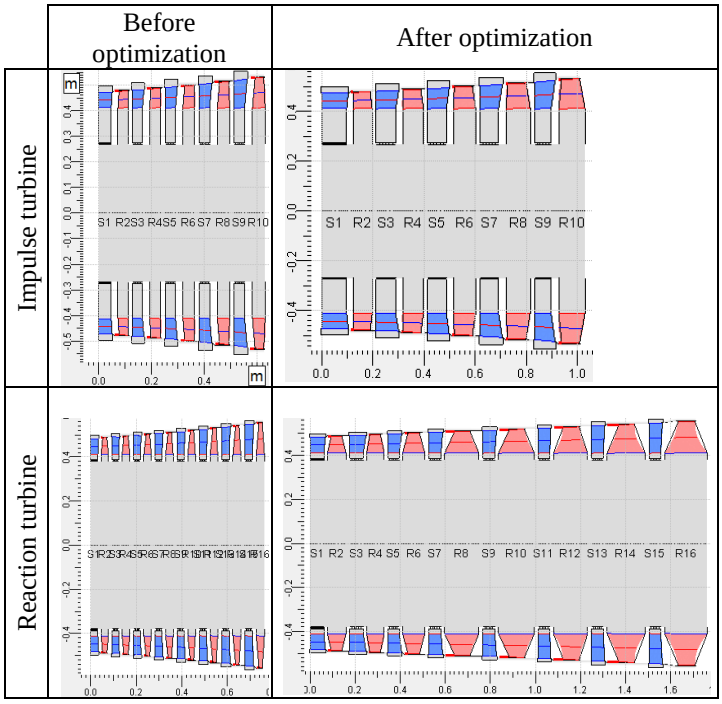

Fig. 9. Comparison of impulse and reaction turbines before and after aero-structural optimization procedure.

Tab. 5. Impulse turbine parameters before and after aero-structural optimization

Stage #	Impulse	
	Before optimization	After optimization
η_{ts}, %	93.69	93.5
N, MW	159.5	159.1
Axial load, MN	0.55	0.54
Axial length, mm	589	1030

Tab. 6. Reaction turbine parameters before and after aero-structural optimization

Stage #	Reaction	
	Before optimization	After optimization
η_{ts}, %	95.5	94.96
N, MW	162.25	161.1
Axial load, MN	1.91	1.83
Axial length, mm	762	1762

The overall length of the impulse turbine increased almost twice, resulting in 1030 mm after aero-structural optimization instead of 589 mm before.

The overall length of the reaction turbine increased even more - 2.3 times - and finally totaled to 1762 mm instead of 762 mm.

Such a significant change in axial length, obtained from aero-structural optimization of flow path geometry, was a result of very high power density, specific for S-CO2 power units, which should be taken into account for turbomachinery design.

Higher blade chords for the reaction turbine were selected to compensate for the higher bending moments (these were caused by higher pressure drops due to higher reaction). The increase of chords from inlet to outlet was caused by a bending moment increase due to a bigger arm (blade height).

CONCLUSIONS

Some aspects of turbomachinery design, specific to S-CO2 power unit's development, were studied and discussed in this article.

The reaction flow path proved to be more efficient than the impulse one. The total-to-static efficiency difference after aero-structural optimization was about 1.5%. However, some drawbacks were noticed.

The higher number of stages will result in higher manufacturing cost as well as axial length. For considered variants, the total axial length of a reaction turbine was 1.7 times bigger than the impulse one.

Additionally, the reaction turbine type turned out to have higher axial thrust and was more sensitive to radial clearances. The efficiency decreased 1% per 1mm clearance for the impulse type turbine and 2% per 1mm clearance for the reaction type turbine.

Consideration of structural aspects revealed significant effects of a working fluid on turbine configuration. Due to higher density of S-CO2, the stages were more loaded compared to steam/gas turbines. Higher stresses forced usage of longer axial chords, resulting in 2.3 times larger total axial length for the reaction turbine type.

ACKNOWLEDGMENTS

We wish to thank the SoftInWay, Inc. team, who generously contributed their time and effort in the preparation of this work. The strength and usability of the material presented here are only as good as the inputs, and their insightful contributions are greatly appreciated.

REFERENCES

[1] Steven A. Wright, Thomas M. Conboy and Gary E. Rochau, "Overview of Supercritical CO2 power cycle development at Sandia National Laboratories", 2011 University Turbine Systems Research Workshop, October 25-27, 2011 Columbus, Ohio.

[2] Moisseytsev, A. Sienicki, J. J. "Performance improvement options for the supercritical carbon dioxide Brayton cycle", Nuclear Engineering Division, Argonne National Laboratory, June 6, 2007.

[3] Yang Chen, "Thermodynamic Cycles Using Carbon Dioxide as Working Fluid," Doctoral Thesis, School of Industrial Engineering and Management, Department of Energy Technology, October 2011.

[4] Dostal, V., "A Supercritical Carbon Dioxide Cycle for Next Generation Nuclear Reactors," Dissertation, Massachusetts Institute of Technology, Department of Nuclear Engineering, January 2004.

[5] Boyko A. V., Govorushchenko Y.N., 1989, Theoretical Basis of Axial-Flow Turbines Optimal Design, Kharkov, Visha Shkola (in russian).

[6] Fuller R., Preuss J., Noall J., 2012, Turbomachinery for supercritical CO2 power cycles, Proceedings of ASME Turbo Expo 2012, Copenhagen, GT2012-68735.

[7] Oleg Guriev, Yuriy Govoruschenko, Leonid Moroz, Supercritical CO2 Brayton Cycle. S-CO2 represents an advance in power conversion technology, Turbomachinery International. The Global Journal of Energy Equipment, January/February 2013.

[8] Leonid Moroz, Yuriy Govoruschenko, Petr Pagur, A uniform approach to conceptual design of axial Turbine / compressor flow path, The Future of Gas Turbine Technology. 3rd International Conference, October 2006, Brussels, Belgium.

[9] Leonid Moroz, Yuriy Govoruschenko, Petr Pagur, Axial turbine stages design: 1d/2d/3d simulation, experiment, optimization, Proceedings of ASME Turbo Expo 2005, Reno-Tahoe, Nevada, USA, GT2005-68614.

[10] Lee J., Ahn Y., Lee J., Yoon H, "Design methodology of supercritical CO2 Brayton cycle turbomachines" Proceedings of ASME Turbo Expo 2012, Copenhagen, GT2012-68933

[11] Pecnic R., Rinaldi E., Colonna P., "Computational fluid dynamics of a radial compressor operating with a supercritical CO2", Proceedings of ASME Turbo Expo 2012, Copenhagen, GT2012-69640.

[12] Gregory A. Johnson, Michael W. McDowell, George M. O'Connor, Chandrshekhar G.Sonwane, Ganesan Subbaraman, "Supercritical CO2 Cycle development at Pratt&Whitney Rocketdyne", Proceedings of ASME Turbo Expo 2012, Copenhagen, GT2012-70105.